

ONCOGENOMICS

***PRTFDC1*, a possible tumor-suppressor gene, is frequently silenced in oral squamous-cell carcinomas by aberrant promoter hypermethylation**

E Suzuki^{1,2}, I Imoto^{1,3,4}, A Pimkhaokham^{1,5}, T Nakagawa¹, N Kamata⁶, K-i Kozaki^{1,3,4}, T Amagasa² and J Inazawa^{1,3,4,7}

¹Department of Molecular Cytogenetics, Medical Research Institute and School of Biomedical Science, Tokyo Medical and Dental University, Tokyo, Japan; ²Department of Maxillofacial Surgery, Graduate School, Tokyo Medical and Dental University, Tokyo, Japan; ³Hard Tissue Genome Research Center, Tokyo Medical and Dental University, Tokyo, Japan; ⁴Core Research for Evolutional Science and Technology (CREST) of Japan Science and Technology Corporation (JST), Saitama, Japan; ⁵Faculty of Dentistry, Department of Oral & Maxillofacial surgery, Chulalongkorn University, Patumwan, Bangkok, Thailand; ⁶Division of Cervico-Gnathostomatology, Department of Oral and Maxillofacial Surgery, Graduate School of Biomedical Sciences, Hiroshima University, Minami-ku, Hiroshima, Japan and ⁷21st Century Center of Excellence Program for Molecular Destruction and Reconstitution of Tooth and Bone, Tokyo Medical and Dental University, Tokyo, Japan

Array-based comparative genomic hybridization (array-CGH) has good potential for the high-throughput identification of genetic aberrations in cell genomes. In the course of a program to screen a panel of oral squamous-cell carcinoma (OSCC), cell lines for genomic copy-number aberrations by array-CGH using our in-house arrays, we identified a 3-Mb homozygous deletion at 10p12 in 1 of 18 cell lines (5.6%). Among seven genes located within this region, expression of *PRTFDC1* mRNA was not detected in 50% (9/18) or decreased in 5.6% (1/18) of OSCC cell lines, but detected in normal oral epithelia and restored in gene-silenced OSCC cells without its homozygous loss after treatment with 5-aza-2'-deoxycytidine. Among 17 cell lines without a homozygous deletion, the hypermethylation of the *PRTFDC1* CpG island, which showed promoter activity, was observed in all nine cell lines with no or reduced *PRTFDC1* expression (52.9%). Methylation of this CpG island was also observed in primary OSCC tissues (8/47, 17.0%). In addition, restoration of *PRTFDC1* in OSCC cells lacking its expression inhibited cell growth in colony-formation assays, whereas knockdown of *PRTFDC1* expression in OSCC cells expressing the gene promoted cell growth. These results suggest that epigenetic silencing of *PRTFDC1* by hypermethylation of the CpG island leads to a loss of *PRTFDC1* function, which might be involved in squamous cell oral carcinogenesis.

Oncogene advance online publication, 18 June 2007; doi:10.1038/sj.onc.1210589

Keywords: array-CGH; oral squamous-cell carcinoma; *PRTFDC1*; homozygous deletion; methylation

Introduction

Oral cancer, predominantly oral squamous-cell carcinoma (OSCC), is the most common head and neck neoplasm, affecting 270 000 people worldwide each year (Parkin *et al.*, 2005). Despite recent progress in the diagnosis of and therapeutic modalities for OSCC, the prognosis has not been improved, reflecting the ineffectiveness of current treatment regimens (Parkin *et al.*, 2005). A more comprehensive understanding of the molecular pathogenesis of OSCC is urgently needed to identify new targets and strategies for effective therapy, and the opportunity to recognize early OSCC and/or premalignant lesions may provide insight into the phase of new strategies for chemoprevention of this disease (Nagpal and Das, 2003; Brinkman and Wong, 2006). Although OSCC is believed to arise through the accumulation of numerous genetic and epigenetic alterations, which may impair the function of oncogenes or tumor suppressor genes (TSGs) that play a crucial role in the development of this disease (Scully *et al.*, 2000; Ha and Califano, 2006), little is still known about the genes associated with oral carcinogenesis.

Although several TSGs, such as *SMAD4*, *RBI*, *PTEN* and *p16INK4A*, were originally identified from homozygous deletions in cancer cells (Friend *et al.*, 1986; Kamb *et al.*, 1994; Hahn *et al.*, 1996; Li *et al.*, 1997), genetic and epigenetic mechanisms other than homozygous loss could contribute to the loss of function of TSGs in tumors. Indeed, epigenetic inactivation of TSGs, including DNA hypermethylation in their CpG-rich promoter or exonic regions, has been believed to occur frequently and play important roles during the pathogenesis of human cancers, including oral cancer (Jones and Baylin, 2002; Ha and Califano, 2006). Hence, the mapping of homozygous deletions in OSCCs using high-throughput methods with high-resolution and sensitivity and further analyses of frequently inactivated 'driver genes' located within mapped regions may provide valuable clues for exploring OSCC-associated

Correspondence: Dr J Inazawa, Department of Molecular Cytogenetics, Medical Research Institute, Tokyo Medical and Dental University, 1-5-45 Yushima, Bunkyo-ku, Tokyo 113-8510, Japan.

E-mail: johinaz.gen@mri.tmd.ac.jp

Received 4 December 2006; revised 12 April 2007; accepted 15 May 2007

TSGs, even those whose inactivation occurs mainly by epigenetic mechanisms. Studies using chromosomal comparative genomic hybridization (CGH) and loss of heterozygosity analyses have attempted to identify copy-number alterations in a genome-wide manner, but are limited by the low resolution or the limited coverage of these technologies as a method to identify homozygous deletions. Array-based CGH (array-CGH) technique allows high-throughput and quantitative analyses of copy-number changes at high-resolution throughout the genome, providing many advantages, including the identification of homozygous loss, over conventional methods (Snijders *et al.*, 2001; Inazawa *et al.*, 2004), although the resolution fully depends on the type of array. Indeed, our previous array-CGH studies using in-house bacterial artificial chromosome- (BAC-)/P1-derived artificial chromosome- (PAC-) based arrays (BAC/PAC-arrays) have successfully mapped complete genetic losses, allowing the rapid identification of candidate TSGs inactivated mainly by genetic and/or epigenetic mechanisms (Sonoda *et al.*, 2004; Izumi *et al.*, 2005; Takada *et al.*, 2005b, 2006; Imoto *et al.*, 2006).

In the study reported here, we identified *PRTFDC1* at 10p12 as a candidate target for a homozygously deleted region detected by array-CGH analyses using in-house BAC/PAC-arrays (MCG Cancer Array-800 and MCG Whole Genome Array-4500) against a panel of OSCC cell lines. Interestingly, expression of this gene was frequently silenced in OSCC cell lines without its homozygous loss, although it was present in normal oral mucosa, suggesting that *PRTFDC1* may be inactivated epigenetically in a cancer-specific manner and contribute to oral carcinogenesis. To assess this hypothesis, we examined the role of DNA methylation within the CpG island around exon 1 of *PRTFDC1* in regard to its expression in OSCC and tested the effect of *PRTFDC1* expression on the growth of OSCC cells.

Results and discussion

In array-CGH analyses using MCG Cancer Array-800 and MCG Whole Genome Array-4500 arrays covering an entire genome with 5323 BAC/PAC clones, copy-number gains and losses were seen to some degree in all of the 18 OSCC cell lines examined (Figure 1a). Since the most common genetic aberrations had already been detected in OSCC cell lines and primary tumors by conventional CGH (Hermsen *et al.*, 1997; Wolff *et al.*, 1998), here, we paid attention to more remarkable patterns of chromosomal abnormalities, such as high-level amplifications and homozygous deletions, which are likely to be landmarks of oncogenes and TSGs, respectively (Baldwin *et al.*, 2005; Snijders *et al.*, 2005). Tables 1 and 2 summarize the clones showing high-level amplifications (\log_2 ratio >2.0) or homozygous deletions (\log_2 ratio <-2.0), respectively.

High-level amplifications were detected in 10 of the 18 OSCC cell lines (55.6%), and 15 cells were represented (Table 1). Among them, 7p11.2 containing *EGFR* is the only region amplified in more than two cell lines (four

lines). On the other hand, two homozygous deletions were identified as novel loci for candidate TSGs in 2 of the 18 OSCC cell lines (Table 2). Although homozygous deletions of *CDKN2A*, a known tumor suppressor gene, at 9p21 have been detected by genomic PCR analysis in HOC-313, HOC-815 and OM-1 previously (Akanuma *et al.*, 1999), our array-CGH analysis failed to detect this alteration probably, because the deletion was too small to be detected with the BAC/PAC-based array. We found a homozygous deletion at 2q24.1–q24.2 in the HO-1-N1 cell line; the region contains no genes whose expression decreased frequently in OSCC cell lines compared with normal oral epithelium (data not shown). In HSC-6 cells, we detected homozygous loss at 10p12. Since the region has been frequently involved in the loss of genetic material in primary OSCC (Jin *et al.*, 2006), we focused on homozygous loss at 10p12 in HSC-6 to examine whether a TSG(s) related to the oral tumorigenesis might lie within this region.

Identification of gene(s) involved in the homozygous deletion at 10p12

To identify all potential target genes for the homozygous deletion at 10p12 in HSC-6 cells, we first tried to define the homozygously deleted region by genomic PCR using this cell line. The maximum extent of the homozygous deletion estimated from the result obtained with the array-CGH was approximately 2.95 Mb (Figures 1b and 2a), and information archived by human genome databases (<http://www.ncbi.nlm.nih.gov/> and <http://genome.ucsc.edu/>) indicated that seven genes are located in this region (Figure 2a). Among them, homozygous losses of *PRTFDC1*, *c10orf63*, *THNSL1*, *GPR158*, *MYO3A* and *GAD2* (white arrows in Figure 2a) were detected in only HSC-6 cells (1/18, 5.6%; Figure 2b), whereas *ARHGAP21* (black arrows in Figure 2a) was retained, narrowing down the region deleted to approximately 1.5 Mb (white closed arrow in Figure 2a).

Frequent loss of PRTFDC1 mRNA expression in OSCC cell lines

Next we determined expression levels of six genes, *PRTFDC1*, *c10orf63*, *THNSL1*, *GPR158*, *MYO3A* and *GAD2*, by means of reverse transcription (RT)-PCR in all 18 OSCC cell lines, RT7, an immortalized cell line derived from normal oral epithelial cells (Fujimoto *et al.*, 2002), and primary cultured normal oral mucosa. The HSC-6 cell line as well as another eight lines without homozygous loss at 10p12 (9/18, 50%) completely lacked expression of *PRTFDC1* mRNA; one line, HOC-313, (1/18, 5.6%) showed reduced expression compared with RT7 and/or primary cultured normal oral mucosa (Figure 2c and Supplementary Figure S1). No mutation was detected in any of coding exons of *PRTFDC1* in all of cell lines tested except HSC-6 with homozygous loss of this gene (data not shown). On the other hand, the expression of *c10orf63*, *THNSL1* and *GPR158* was absent less frequently (Figure 2c), and

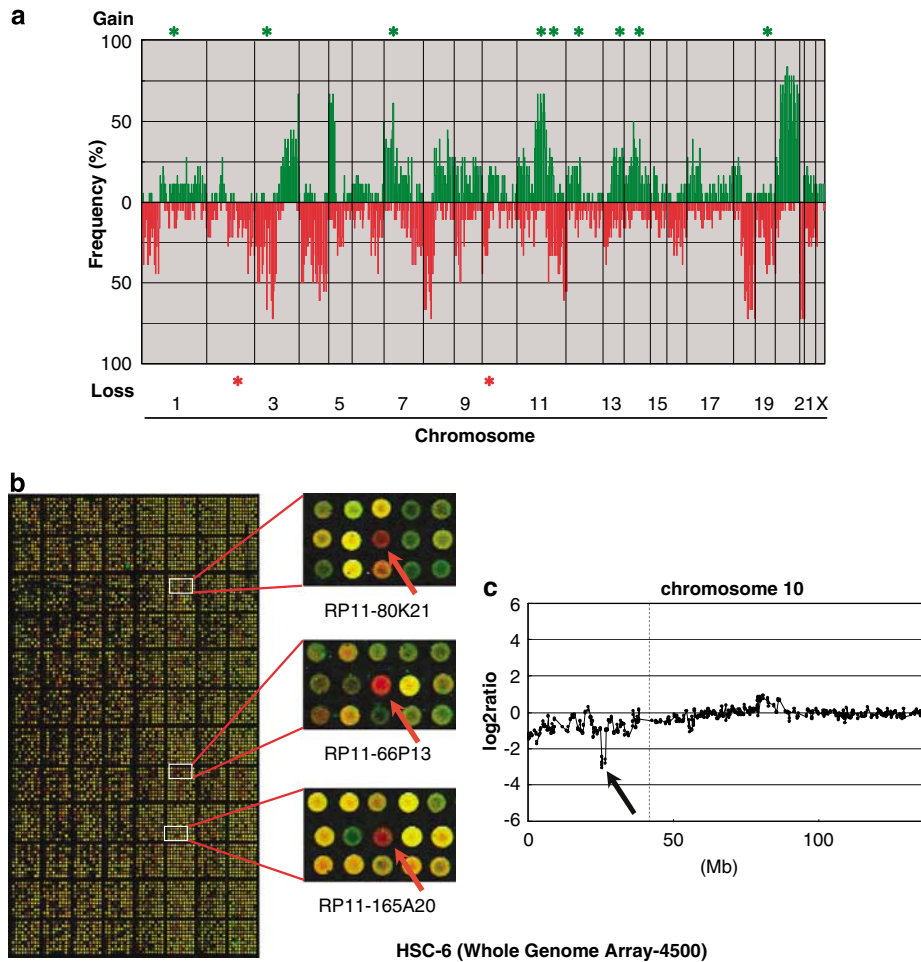


Figure 1 (a) Genome-wide frequencies of copy-number gains (above 0, green) and losses (below 0, red) detected by MCG Cancer Array-800 in 18 oral squamous-cell carcinoma cell lines. Clones are ordered from chromosomes 1–22, X and Y and within each chromosome on the basis of the UCSC mapping position (<http://genome.ucsc.edu/> (version May, 2004)). Green asterisks (*), regions with high-level amplification (\log_2 ratio > 2); red asterisks (*), regions with homozygous deletion (\log_2 ratio < -2) detected with either MCG Cancer Array-800 or MCG Whole Genome Array-4500. (b) Representative duplicate array-based comparative genomic hybridisation image (MCG Whole Genome Array-4500) of the HSC-6 cell line. A remarkable decrease in copy-number ratio (\log_2 ratio < -2) of RP11-165A20, 80K21 and 66P13 (red arrows) at 10p12 was detected as a clear red signal. (c) Representative copy-number profiles of chromosome 10 in HSC-6 cells. The vertical back bar indicates candidate spots showing patterns of homozygous deletion at 10p12 (\log_2 ratio < -2).

GPR158 was not expressed in RT7 and primary cultured normal oral mucosa. In coding sequences of *c10orf63* and *THNSL*, no mutation was also detected in all of cell lines tested except HSC-6 (data not shown). *MYO3A* and *GAD2* were not expressed in RT7 and primary cultured normal oral mucosa probably due to their tissue-specific expression pattern, which is also described in expression databases (<http://www.ncbi.nlm.nih.gov/> and <http://www.lsbm.org/database/index.html>), although these genes were not expressed in any of the OSCC cell lines (data not shown). Those results prompted us to focus on the *PRTFDC1* gene as the most likely target for inactivation within the homozygously deleted region at 10p12, and suggest that frequent loss of *PRTFDC1* mRNA expression in OSCC cell lines might result from mechanisms other than genomic deletion or mutation, including epigenetic events.

Effect of demethylation by 5-aza-2'-deoxycytidine on PRTFDC1 expression

Aberrant methylation of DNA within promoter regions harboring a larger than expected number of CpG dinucleotides is a key mechanism by which TSGs can be silenced (Jones and Baylin, 2002). To investigate whether demethylation could restore expression of *PRTFDC1* mRNA, we treated OSCC cells lacking *PRTFDC1* expression (ZA, NA and HSC-2) with 5-aza-2'-deoxycytidine (5-aza-dCyd), a methyltransferase inhibitor, for 5 days. *PRTFDC1* mRNA was expressed in all cell lines after treatment with 5-aza-dCyd (Figure 2d). On the other hand, treatment with trichostatin A (TSA), a histone deacetylase inhibitor, alone had no effect on the expression of *PRTFDC1*. In addition, no enhancement of *PRTFDC1* expression by 5-aza-dCyd given along with TSA was observed, indicating that histone deacetylation may play a minimal role in the

Table 1 High-level amplifications (log2 ratio > 2.0) detected in OSCC cell lines by array-CGH analysis using MCG Cancer Array-800 and Whole Genome Array-4500

No	BAC	Locus ^a		Cell line (total 18)		Possible candidate gene ^b	Number of known gene
		Chromosome band	Position	n	Name		
1	RP11-123P3	1q21	chr1:144,160,737-144,316,863	1	HSC-7	<i>BCL9</i>	38
	RP11-433J22		chr1:144,332,334-144,519,348		HSC-7		
	RP11-444P10		chr3:69,701,828-69,903,040		HSC-7		
2	RP11-215K24	3p13	chr3:70,082,272-70,235,455	1		<i>MITF</i>	20
	RP11-90H15		chr3:71,172,843-71,304,638				
	RP11-154H23		chr3:71,622,959-71,816,508				
3	RP11-14K11	7p11.2	chr7:54,903,388-54,903,650	4	ZA, NA, HSC-2, KON	<i>EGFR</i>	9
	RP11-339F13		chr7:55,029,594-55,154,846				
	RP11-97P11		chr7:55,238,305-55,381,999				
4	RP11-34J24	11p15.4	chr7:55,274,090-55,403,627	1	OM-1	<i>PTH</i>	62
	RP11-120E20		chr11:3,573,460-3,758,006				
	RP11-350M7		chr11:13,284,758-13,494,094				
5	RP11-300I6	11q13.3	chr11:69,162,462-69,323,966	1	OM-1	<i>BCL1, FGF4, CCND1, FGF3</i>	40
	CTD-2234J21		chr11:69,307,612-69,307,884				
	RP11-804L21		chr11:100,365,386-100,536,934				
7	RP11-68I017	11q22	chr11:101,517,505-101,686,954	1	TSU	<i>PGR, YAPI, CIAP1, MMP7, MMP1</i>	31
	RP11-111A13		chr11:101,600,598-101,786,581				
	RP11-864G5		chr11:101,724,636-101,939,137				
8	RP11-315O6	11q23.3	chr11:102,010,611-102,191,046	2	OM-1, NA	<i>CCND2, FGF6</i>	3
	RP11-750P5		chr11:102,613,696-102,771,594				
	RP11-2122		chr11:119,773,356-119,939,639				
9	CTD-2058B01	12p13	chr12:2,977,826-3,145,569	1	HSC-7		33
	RP11-24N12		chr12:3,295,578-3,473,577				
	RP11-88D16		chr12:4,177,493-4,279,837				
10	RP11-74M9	12q24.31	chr12:4,313,654-4,483,853	1	HSC-5	<i>BCL7A</i>	56
	RP11-388F6		chr12:120,771,781-120,958,360				
	RP11-87C12		chr12:121,153,004-121,339,958				
11	RP11-512 M8	13q33.3-q34	chr13:109,059,437-109,253,923	1	HSC-7	<i>DPI, GAS6</i>	99
	RP11-313L9		chr13:110,332,616-110,333,140				
	RP11-91C11		chr13:113,193,310-113,252,507				
12	RP11-230F18	14q24.1	chr13:113,492,714-113,658,045	1	NA		25
	RP11-51H10		chr14:68,410,041-68,581,432				
	RP11-74M3		chr14:69,101,595-69,152,329				
13	RP11-59M15	19q13	chr14:69,266,041-69,440,807	1	SKN-3	<i>SUPT5H</i>	99
	RP11-72J8		chr14:69,652,605-69,652,944				
	RP11-18G18		chr19:43,015,766-43,182,195				
14	RP11-91H20	22q12.1	chr19:43,372,949-43,537,375	1	HSC-7		13
	RP11-140E1		chr19:43,861,826-43,880,848				
	RP11-118P21		chr19:44,156,778-44,353,574				
14	RP11-446K10	22q12.1	chr19:44,449,022-44,620,150	1	HSC-7		13
	RP11-67A5		chr19:44,586,344-44,776,946				
	RP11-256O9		chr22:24,445,961-24,605,516				
RP11-89A2	chr22:24,942,081-24,951,525						

Abbreviations: Array-CGH, array-based comparative genomic hybridization; BAC, bacterial artificial chromosome; OSCC, oral squamous-cell carcinoma. ^aBased on UCSC Genome Browser, May 2004 Assembly. ^bRepresentative candidate oncogene located around BAC.

Table 2 Homozygous deletions ($\log_2\text{ratio} < -2.0$) detected in OSCC cell lines by array-CGH analysis using MCG Cancer Array-800 and Whole Genome Array-4500

No	BAC	Locus ^a		Cell line (total 18)		Possible candidate gene ^b	Number of known gene
		Chromosome band	Position	n	Name		
1	RP11-91K6	2q24.1-q24.2	chr2:159,678,005-159,832,799	1	HO-1-N-1	None	23
2	RP11-165A20	10p12.1	chr10:25,269,606-25,426,074	1	HSC-6	None	17
	RP11-80K21		chr10:25,407,097-25,570,777				
	RP11-66P13		chr10:26,528,582-26,697,629				

Abbreviations: Array-CGH, array-based comparative genomic hybridization; BAC, bacterial artificial chromosome; OSCC, oral squamous-cell carcinoma. ^aBased on UCSC Genome Browser, May 2004 Assembly. ^bGenes located around BAC, whose homozygous deletion was validated by genomic PCR.

transcriptional silencing of *PRTFDC1* among OSCC cells.

Promoter activity of the *PRTFDC1* CpG island

A 801-bp sequence around exon 1 of *PRTFDC1* (Figure 3a) was identified as a CpG island by using the genome database (<http://www.ebi.ac.uk/emboss/cpgplot/>). To determine whether hypermethylation of CpG sites is associated with transcriptional silencing of the *PRTFDC1* gene, we tested the promoter activity of this CpG island in OSCC cells (NA and HSC-2) using a 891-bp fragment (Fragment 1) covering the entire CpG island and 482-bp (Fragment 2) and 409-bp (Fragment 3) fragments covering uncommonly and commonly methylated regions, respectively, in cell lines without expression of *PRTFDC1* (Figures 3a and b). We observed a remarkable increase in transcriptional activity of the reporter plasmid containing Fragments 1 and 3 compared with the mock reporter plasmid and reporter plasmid containing Fragment 2 in the plasmid-containing cell lines (Figure 3b), suggesting that the CpG island around exon 1 of *PRTFDC1*, especially the region commonly methylated in *PRTFDC1*-nonexpressing cell lines, contains promoter activity, although few studies, including ours, have shown that promoter activity can be observed in fragments, especially CpG islands, not containing a 5' sequence around transcriptional start sites (Kolb 2003; Nakagawachi *et al.*, 2003; Sonoda *et al.*, 2004; Misawa *et al.*, 2005).

Methylation status of the *PRTFDC1* CpG island in OSCC cell lines and primary tumors

To clarify the role of methylation within the *PRTFDC1* CpG island on the expression level of this gene, we first assessed the methylation status of this CpG island in OSCC cell lines with or without expression of this gene, by means of a combined bisulfite restriction analysis (COBRA) using appropriate restriction enzymes for each of the two PCR fragments covering the entire CpG island (Regions 1, 2 in Figure 3a). OSCC cell lines with clear *PRTFDC1* expression (TSU, HOC-815, HSC-4, HSC-5, HSC-7, SKN-3, HO-1-N-1 and KOSC-2) and RT7 tended to be dominantly hypomethylated in both regions (Figure 3c). In nine OSCC cell lines that showed no or reduced *PRTFDC1* expression without a homozygous deletion, on the other hand, dominant

hypermethylation was observed in either of the regions, especially Region 2 (Figure 3c), which overlaps the sequence with significant promoter activity *in vitro* (Figure 3b), suggesting that methylation of CpG sites around Region 2 may play an important role in the silencing of *PRTFDC1* expression. Since three of those nine cell lines (OM-2, ZA and NA; Supplementary Table S1) showed a hemizygous deletion pattern within the 10p12 region in our array-CGH analysis ($\log_2\text{ratio} < -0.4$), biallelic methylation or monoallelic methylation with loss of the heterozygous allele may be important for inactivating *PRTFDC1* in OSCC, although its inactivation occurs mainly through the former mechanism.

To assess the methylation status of each CpG dinucleotide within the *PRTFDC1* CpG island in more detail, we performed bisulfite sequencing in cell lines with or without the expression of *PRTFDC1* (Figure 3d). CpG sites on the CpG island tended to be highly methylated in *PRTFDC1*-nonexpressing OSCC cells without homozygous deletion (ZA, HSC-2), whereas almost all CpG sites were unmethylated in one of the *PRTFDC1*-expressing OSCC cell lines (KOSC-2) and, in control RT7 cells. Notably, *PRTFDC1* expression was retained in cell lines having alleles in which almost all the CpG sites were unmethylated (HOC-313 in Figure 3d), although % methylation in this line was similar to that in the cell line lacking *PRTFDC1* expression (ZA in Figure 3d). A similar finding was observed in DNA from ZA and HSC-2 cells treated with 5-aza-dCyd (Figure 3d); those cells showed entirely unmethylated and partially or entirely methylated alleles simultaneously within the *PRTFDC1* CpG island and restored *PRTFDC1* mRNA expression after treatment with 5-aza-dCyd. Those findings suggest that an allele with almost entirely unmethylated CpG sites, especially in Region 2, through the CpG island might be needed for *PRTFDC1* mRNA to be fully expressed.

Methylation status of the *PRTFDC1* CpG island in primary tumors of OSCC

To determine whether hypermethylation of the *PRTFDC1* CpG island also takes place in primary tumors of OSCC, we carried out COBRA using 47 cases of OSCC (Figure 4a). Methylated alleles in the *PRTFDC1* CpG

island were observed in 8 of 47 samples (17.0%), whereas the unmethylated allele was observed in all cases probably due to unavoidable contamination by noncancerous cells. Since the DNAs had been isolated from snap-frozen tumors, the lower frequency of methylation in primary tumors compared with cell lines could also reflect contamination of the specimens with noncancerous cells, leading to underestimation. To validate the methylation status of primary tumors in a more quantitative manner, we next performed bisulfite sequencing in some of the primary cases, and confirmed the more or less methylated CpG sites in COBRA-positive OSCC tissues (cases 68, 69 and 75, Figure 4b). As a result, hypomethylated alleles were also sequenced in COBRA-positive OSCC tissues again, probably owing to the normal tissue components included in tumor tissues (Figure 4b). Since methylated CpG sites in the *PRTFDC1* CpG island were observed in primary OSCCs as well whereas the normal epithelial cell-derived cell line RT7 showed hypomethylation in this

CpG island (Figures 3c and d), methylation of the *PRTFDC1* CpG island did not arise during the passage of OSCC cell lines *in vitro*, but rather may be a true cancer-related event during oral carcinogenesis, although normal oral tissue corresponding to each tumor was not available to further confirm this supposition.

To determine the significance of the *PRTFDC1* CpG island's methylation in the pathogenesis of OSCC, we first analysed the relationship between methylation status within Region 2 of the CpG island determined by COBRA (Figure 3a) and clinicopathological characteristics of all 47 primary tumors. The methylation status of the *PRTFDC1* CpG island in each sample was not associated with gender, age, smoking or drinking history, histologic subtype (differentiation status), or tumor staging, although data were not fully available for some of those variables and only three cases of early stage tumor (stage I) were available for analysis (Table 3). Consequently, the methylation status of *PRTFDC1* is unlikely to correlate with tumor behavior, although information on patient outcome was not available. However, among various TSGs, such as *CDKN2B* and *2A*, *CDH1*, *DAPK1*, *MGMT* and *DCC*, whose methylation is known to be important in the development of OSCC (Ha and Califano, 2006; Shaw, 2006), only a few reports have shown a correlation between the methylation status of those genes and clinicopathological characteristics or prognosis (Shaw, 2006). Since there may be the potential for therapeutic and/or diagnostic advantages if specific aberrations could be shown to correlate with tumor behavior, further study using a larger set of cases, especially early

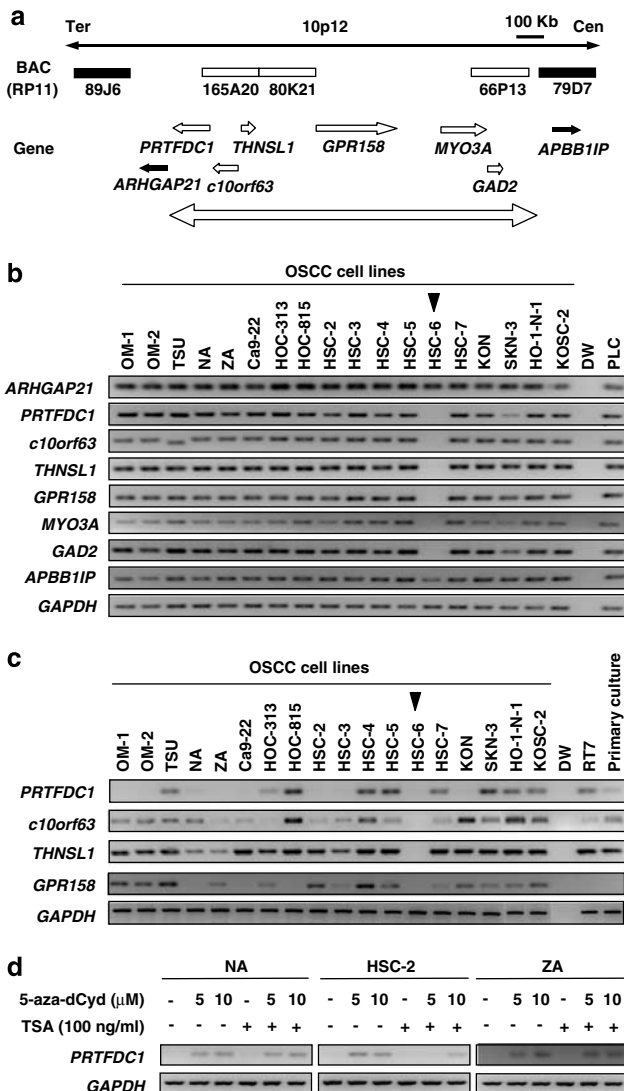


Figure 2 (a) Map of 10p12 covering the region homozygously deleted in the HSC-6 cell line. Bacterial artificial chromosomes (BACs) spotted on the array are shown by horizontal bars: white bars, BACs with log₂ ratio < -2 indicating homozygous deletion; black bars, BACs with log₂ ratio > -2 in HSC-6 cells. The minimum homozygously deleted region in HSC-6 cells, as determined by genomic PCR, is indicated as a horizontal white closed arrow. Eight genes located around this region, which are homozygously deleted (six genes) or retained (two genes) detected by genomic PCR in the HSC-6 cell line, are indicated as white or black bars, respectively, that show positions and directions of transcription. (b) Images from genomic PCR experiments showing *GAPDH*, the functional control and eight genes that were harbored around the homozygous deletion at 10p12 using 18 oral squamous-cell carcinoma (OSCC) cell lines including HSC-6. DW, distilled water; PLC, normal peripheral lymphocytes. The arrowhead indicates the cell line having the homozygous deletion at 10p12 (HSC-6). (c) Expression of *PRTFDC1*, *c10orf63*, *THNSL1*, *GPR158*, *MYO3A* and *GAD2* in OSCC cell lines, and control RT7 and primary culture of normal oral epithelial cells, detected by RT-PCR. DW, distilled water. Arrowhead indicates the cell line (HSC-6) with the homozygous deletion shown in (b). Note that eight (OM-1, OM-2, NA, ZA, Ca9-22, HSC-2, HSC-3 and KON) of the 18 cell lines without a homozygous deletion of *PRTFDC1* showed almost complete silencing of this gene and one line (HOC-313) showed decreased expression compared with normal controls. (d) Representative results of RT-PCR analysis to reveal *PRTFDC1* expression in NA, HSC-2 and ZA cells with or without treatment with 5-aza-dCyd (5 or 10 μM) for 5 days and/or TSA (100 ng/ml) for 24 h.

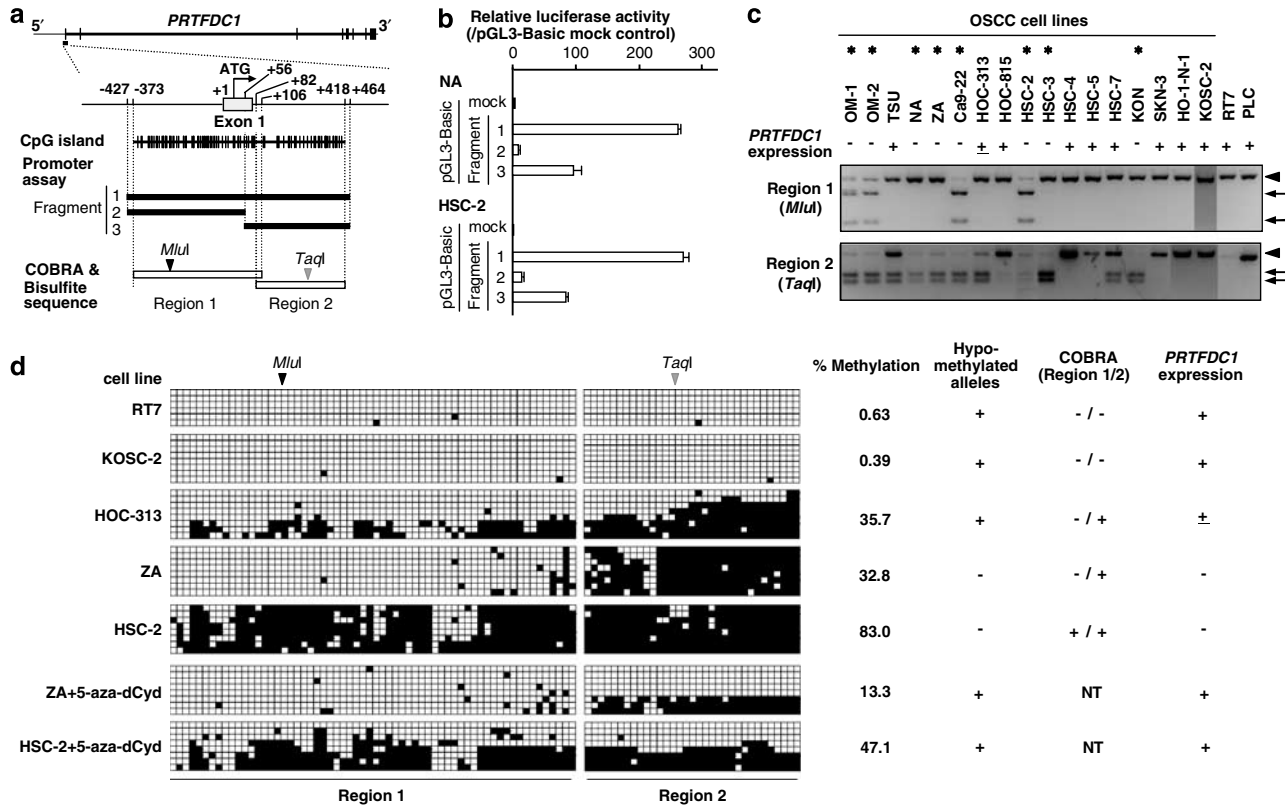


Figure 3 (a) Schematic map of the 801-bp CpG island (-373 to +418) around exon 1 of the *PRTFDC1* gene. CpG sites are indicated by vertical ticks on the expanded axis. Exon 1 is indicated by an open box, and the transcription start site is marked at +1. The fragment (Fragments 1-3) examined in a promoter assay is indicated by heavy black lines. The regions examined in COBRA and bisulfite-sequencing (Regions 1 and 2) are indicated by horizontal open bars. For COBRA, restriction sites for *MluI* and *TaqI* are indicated respectively by black or gray downward arrowheads. (b) Promoter activity of the *PRTFDC1* CpG island. pGL3 basic empty vectors (mock) or constructs containing Fragments 1, 2, or 3 around exon 1 of *PRTFDC1* (Figure 3a) were transfected with an internal control vector (pRL-hTK) into NA and HSC-2 cells. Luciferase activities were normalized versus an internal control. The data presented are the means \pm s.d. of three separate experiments, each performed in triplicate. (c) Representative results of COBRA of *PRTFDC1* Region 1 and Region 2 in a panel of oral squamous-cell carcinoma cell lines after digestion with *MluI* and *TaqI*, respectively. Arrows show fragments specifically restricted in the sites recognized as methylated CpGs. An arrowhead indicates the unrestricted (unmethylated) fragment. As indicated by asterisks (*), eight cell lines were positive for restricted DNA fragments. (d) Results of bisulfite sequencing of the *PRTFDC1* Region 1 (62 CpG sites) and Region 2 (33 CpG sites), examined in *PRTFDC1*-expressing and -nonexpressing cell lines. Each square indicates a CpG site: open squares, unmethylated; solid squares, methylated. Percent of solid squares in all squares analysed in each cell line was indicated by %methylation. NT, not tested.

stage tumors, will be necessary for those methylation-target genes including *PRTFDC1* in OSCC.

Suppressive effect of *PRTFDC1* expression on cell growth of OSCC cells

To gain further insight into the potential role of *PRTFDC1* protein in oral carcinogenesis, we investigated whether restoration of *PRTFDC1* expression would suppress growth of OSCC cells in which the gene had been silenced. We performed colony-formation assays (Sonoda *et al.*, 2004) using the full coding sequence of *PRTFDC1* with a Myc-tag cloned into a mammalian expression vector (pCMV-3Tag4A-*PRTFDC1*) and cells lacking expression of *PRTFDC1*. As shown in Figure 5, 3 weeks after transfection and subsequent selection of drug-resistant colonies, the numbers of large colonies produced by *PRTFDC1*-transfected NA and OM-2 cells decreased compared to those

produced by empty vector-transfected cells. We have not been able to obtain *PRTFDC1*-stable transfectants, which will be useful for further analyses of the tumor-suppressive function, from OSCC cell lines lacking expression of this gene (data not shown).

To confirm a growth-suppressive effect of *PRTFDC1* in OSCC cells and exclude a possible non-specific toxicity of forced-expression of exogenous *PRTFDC1* in colony-formation assay, we knocked down endogenously expressed *PRTFDC1* by transient transfection of *PRTFDC1*-specific synthetic small interfering RNA (siRNA) to HO-1-N-1 and HSC-4 cell lines retaining expression of *PRTFDC1* (Figure 5b). Transfection of *PRTFDC1*-siRNA effectively knockdown of expression level of *PRTFDC1* mRNA compared with *Luc*-siRNA in both cell lines. Transfection of *PRTFDC1*-siRNA accelerated cell growth in those cell lines compared with *Luc*-siRNA transfected counterparts, although the efficiency of growth promoting effect of *PRTFDC1*-siRNA

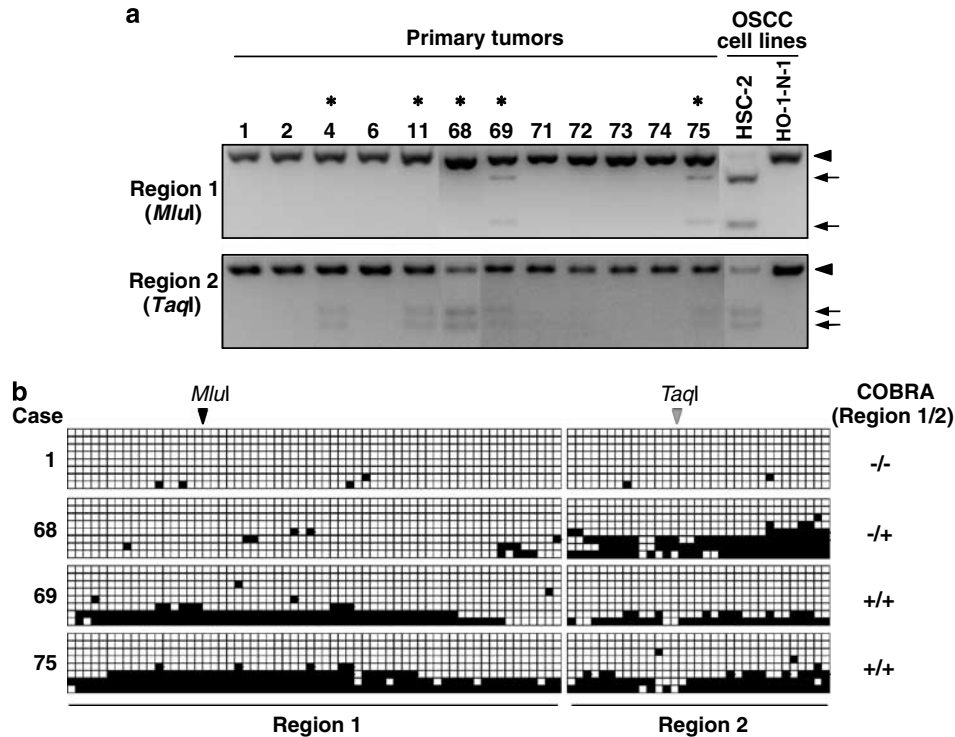


Figure 4 (a) Representative results of COBRA of *PRTFDC1* Region 1 and Region 2 in 12 of 47 primary oral squamous-cell carcinoma (OSCC) tissues (in other 35 samples not shown) with positive (HSC-2) and negative (HO-1-N-1) control cell lines. Primary OSCC cases, which showed positive restricted DNA fragments (Arrows), are indicated by asterisks (*). See the legend for Figure 3c for interpretation. (b) Methylation status of *PRTFDC1* Regions 1 and 2 in four primary cases of OSCC determined by bisulfite sequencing. See the legend for Figure 3d for interpretation.

was different between two cell lines. Since transfection of *PRTFDC1*-siRNA to HSC-6 lacking expression of *PRTFDC1* showed no effect on cell growth compared with *Luc*-siRNA (data not shown), growth promoting effect of *PRTFDC1*-siRNA transfection observed in HO-1-N1 and HSC-4 cell lines may not be caused by off-target effects or simple toxicity of siRNA used in this study. In fluorescence-activated cell sorting (FACS) analysis using HO-1-N-1 cell line, knockdown of *PRTFDC1* resulted in a decrease in G₀-G₁ phase cells and an increase in S and G₂-M phase cells (Figure 5b, lower), suggesting that *PRTFDC1* may arrest OSCC cells at the G₁-S checkpoint.

PRTFDC1 encodes a protein containing a phosphoribosyl transferase domain (<http://www.ncbi.nlm.nih.gov/entrez>). *PRTFDC1* is highly homologous to HPRT1, hypoxanthine phosphoribosyl transferase 1; the mRNA-coding sequence has 68% homology, while the amino-acid sequence is also 68% homologous (Nicklas, 2006). According to the Homologene entry (<http://www.ncbi.nlm.nih.gov/entrez/query.fcgi?db=homologene>), this gene is conserved in vertebrates; this level of conservation implies that *PRTFDC1* must be a functional gene, though its function is unknown. Our colony-formation assays using *PRTFDC1*-transfected OSCC cells and cell growth-assays using *PRTFDC1*-specific siRNA revealed growth-suppressive and/or anti-proliferative activity of the *PRTFDC1* protein; neither had ever been demonstrated before. As no system we tried was successful for obtaining stable

cell lines expressing *PRTFDC1*, it will be difficult to investigate the mechanisms of tumor-suppressing activity of *PRTFDC1* any further. In addition, the expression analysis of *PRTFDC1* mRNA in various human normal tissues was using real-time RT-PCR revealed differential expression pattern of this gene among tissues (Supplementary Figure S1), suggesting that significance of *PRTFDC1* expression in carcinogenesis may be determined in a tissue-/cell-lineage-dependent manner. Since little information is available about the functional consequences of *PRTFDC1*'s inactivation in terms of oral carcinogenesis as well as its substrates and/or physiological functions, additional studies should be designed to solve those issues.

In summary, we performed array-CGH using two types of in-house BAC/PAC-based genome arrays, covering the entire human genome with a total of 5323 BACs, to examine a panel of OSCC cell lines for copy-number alterations within smaller regions. From the homozygously deleted region at 10p12 detected in one cell line, we identified *PRTFDC1* whose expression is frequently silenced as a consequence of DNA methylation within the CpG island having promoter activity and re-expression inhibits growth of OSCC cells lacking its expression, although its functional consequences in carcinogenesis remain unknown. Since methylation of the *PRTFDC1* CpG island was observed in primary OSCC cases as well, future studies should focus on the

Table 3 Relation between clinicopathological data and hypermethylation of the *PRTFDC1* CpG island

	n	<i>PRTFDC1</i> hypermethylation (%) ^a	P ^b
Total	47	8 (17.0)	
<i>Gender</i>			
Male	19	2 (10.5)	0.4448
Female	28	6 (21.4)	
<i>Age</i>			
Median (range)	69.0 (49–90)		
years			
> 60	12	1 (8.3)	0.6593
≤ 60	35	7 (20.0)	
<i>Smoking^c</i>			
Smoker	13	0 (0)	0.1317
Nonsmoker	21	5 (23.8)	
<i>Alcohol^d</i>			
Drinker	10	0 (0)	0.1472
Nondrinker	21	5 (23.8)	
<i>Differentiation^e</i>			
Well-mod	34	6 (17.6)	> 0.9999
Poor	4	1 (25.0)	
<i>TNM classification</i>			
<i>T stage</i>			
T1	3	0 (0)	> 0.9999
T2-4	44	8 (18.2)	
<i>N stage</i>			
N0	32	4 (12.5)	0.2455
N1-3	15	4 (26.7)	
<i>M stage</i>			
M0	40	7 (17.5)	> 0.9999
M1	7	1 (14.3)	
<i>Stage</i>			
I, II	16	3 (18.8)	0.6645
III, IV	31	5 (16.1)	

^aMethylation status was determined by methylation-specific PCR as described in Materials and methods. ^bP-values are from the χ^2 or Fisher exact test and were statistically significant when <0.05 (two-sided). ^cNo information in 13 cases. ^dNo information in 16 cases. ^eNo information in nine cases.

determination of its potential as a marker for the detection of disease as well as disease status, prediction of outcome and sensitivity to chemotherapy.

Materials and methods

Cell lines and primary tumors

A total of 18 OSC cell lines (OM-1, OM-2, TSU, ZA, NA, Ca9-22, HOC-313, HOC-815, HSC-2, HSC-3, HSC-4, HSC-5, HSC-6, HSC-7, KON, SKN-3, HO-1-N-1 and KOSC-2) established from surgically resected tumors in Tokyo Medical and Dental University (Akanuma *et al.*, 1999) or purchased from the Japanese Collection of Research Bioresources (Osaka, Japan) were maintained in Dulbecco's modified Eagle's MEM supplemented with 10% fetal bovine serum, and 100 units/ml penicillin/100 μ g/ml streptomycin. The normal oral epithelial cell-derived cell line, RT7, was maintained in keratinocyte serum-free medium containing epidermal growth factor and bovine pituitary extract (Invitrogen, Carlsbad, CA, USA; Fujimoto *et al.*, 2002).

Primary OSCC tumor samples were obtained during surgery from 58 patients who were treated at the National Cancer Institute or Chulalongkorn University, Bangkok, Thailand, with prior written consent from each patient and approval by

the local ethics committee. None of the patients had been administered preoperative radiation, chemotherapy, or immunotherapy. Tissues from the patients were immediately frozen in liquid nitrogen and stored at -80°C until required. Genomic DNA and/or total RNA were isolated from each cell line or frozen primary tumor according to procedures described elsewhere. As control, we performed a primary culture of oral gingival epithelial cells (Kusumoto *et al.*, 2004), obtained from a non-smoking healthy adult male under the approval for this study. RNA from various human normal tissues was purchased from Clontech (Mountain View, CA, USA).

Array-CGH analysis

Hybridizations were carried out as described elsewhere (Takada *et al.*, 2005a,b) with minor modifications using a hybridization machine (GeneTAC; Harvard Bioscience, Holliston, MA, USA). Hybridized slides were scanned with a GenePix 4000B (Axon Instruments, Foster City, CA, USA) and acquired images were analysed with GenePix Pro 6.0 imaging software (Axon Instruments). Fluorescence ratios were normalized so that the mean of the middle-third of log 2 ratios across the array was zero. Average ratios that deviated significantly (> 2 s.d.) from zero were considered abnormal.

Genomic PCR

We screened DNAs from OSCC lines for homozygous losses by genomic PCR. All the relevant primer sequences are listed in Supplementary Table S2.

RT-PCR and real-time RT-PCR

Single-stranded cDNAs were generated from total RNAs. For RT-PCR, cDNAs were amplified with primers specific for each gene (Supplementary Table S2). The gene encoding glyceraldehyde-3-phosphate dehydrogenase (*GAPDH*) was amplified at the same time to estimate the efficiency of cDNA synthesis.

For real-time RT-PCR, primer set and probe for *PRTFDC1* were purchased from Applied Biosystems (TaqMan Gene Expression Assays; Foster City, CA, USA). The RT-PCR was performed using an ABI PRISM 7500 sequence detection System (Applied Biosystems) according to the manufacturer's instructions. Gene expression values are expressed as ratios (differences between the C_t values) between the genes of interest and an internal reference gene (*GAPDH*) that provides a normalization factor for the amount of RNA isolated from a specimen, and subsequently normalized with the value in the control cells (relative expression level). PCR amplifications were performed in triplicate for each sample.

Mutation analysis

We looked for mutations within coding sequence of each gene by means of exon amplification and direct sequencing, using primers designed for genomic sequences around each exon (Supplementary Table S2). Any base changes detected in samples were confirmed by sequencing each product in both directions.

Drug treatment

Cells were treated with 0, 5, or 10 μM of 5-aza-dCyd for 5 days without or with 100 ng/ml of TSA for the last 24 h.

Promoter reporter assay

A 891-bp fragment (Fragment 1 in Figure 3a) around the CpG island of *PRTFDC1* predicted by the CpGPLOT program

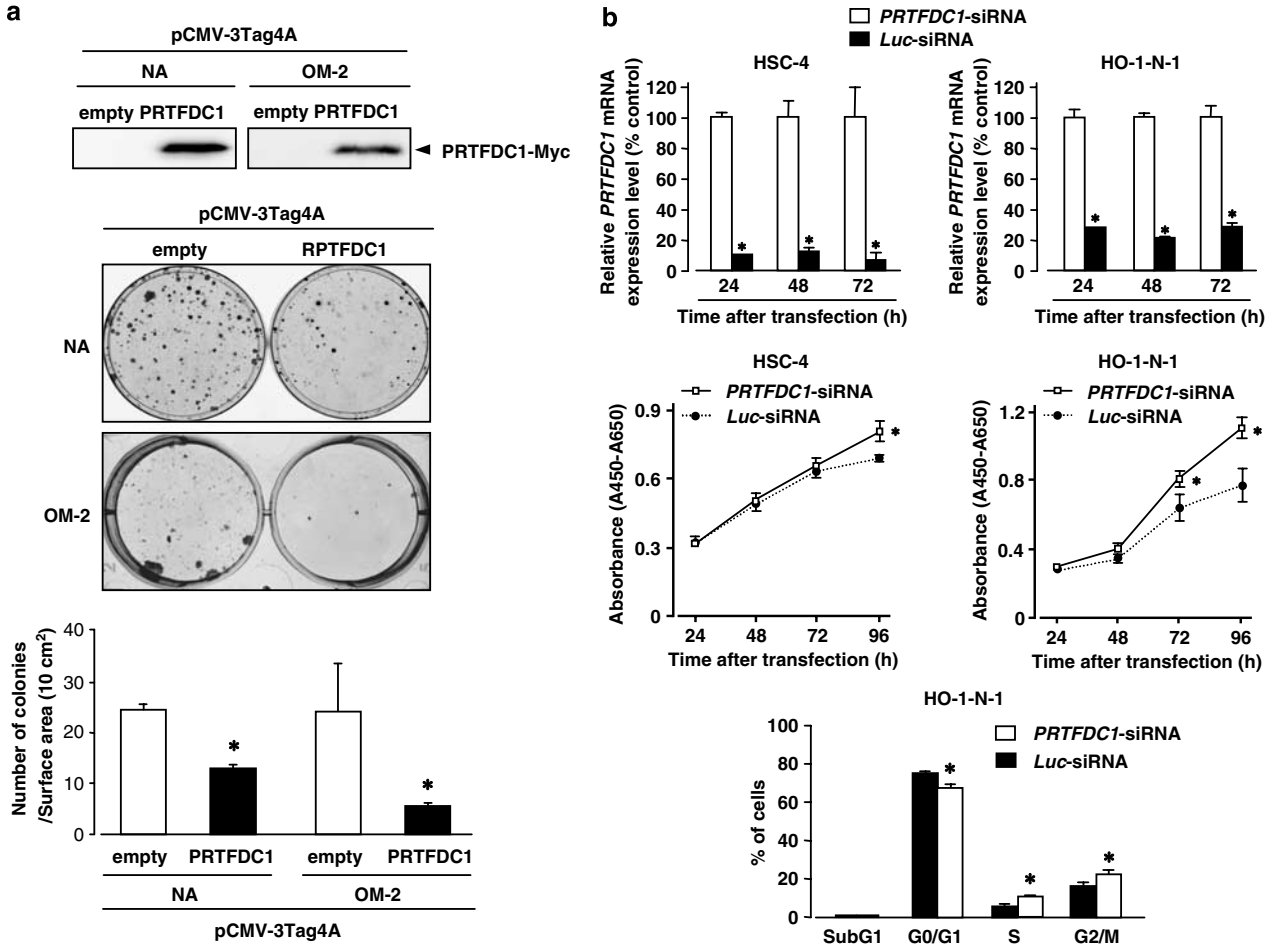


Figure 5 (a) Effect of restoration of *PRTFDC1* on growth of oral squamous-cell carcinoma (OSCC) cells. A Myc-tagged construct containing *PRTFDC1* (pCMV-3Tag4A-*PRTFDC1*) or empty vector (pCMV-3Tag4A-mock) as a control was transfected into NA or OM-2 cells, which lack expression of the *PRTFDC1* gene. Upper: western-blot analysis using 5 μ g of protein extract from cells 48 h after transfection and anti-Myc antibody demonstrated that transiently pCMV-3Tag4A-*PRTFDC1*-transfected cells expressed Myc-tagged *PRTFDC1* protein. Middle: 3 weeks after transfection and subsequent selection of drug-resistant colonies in 6-well plates or 100-mm dishes, the colonies formed by *PRTFDC1*-transfected cells were less numerous than those formed by mock-transfected cells. Lower: quantitative analysis of colony formation. Colonies larger than 2 mm were counted, and results are presented as the means \pm s.d. (bars) of three separate experiments, each performed in triplicate. Statistical analysis used the Mann-Whitney *U*-test: **P* < 0.05 versus empty-vector transfected cells. (b) Effects of knockdown of endogenous *PRTFDC1* on growth of OSCC cells. Upper: Quantitative real-time RT-PCR analysis of *PRTFDC1* mRNA after transfection of 50 nM of *PRTFDC1*-specific small interfering RNA (siRNA) (*PRTFDC1*-siRNA) or a control siRNA for the *luciferase* gene (*Luc*-siRNA) into OSCC cell lines expressing *PRTFDC1* (HO-1-N-1 and HSC-4). Relative expression levels of *PRTFDC1* mRNA in *PRTFDC1*-siRNA-treated cells normalized with those in *Luc*-siRNA-transfected counterparts at indicated times were calculated. Middle: The numbers of viable cells after transfection of 50 nM of each siRNA were assessed at the indicated times by water-soluble tetrazolium salt assay. The data presented are the means \pm s.d. of triplicate experiments. Statistical analysis used the Mann-Whitney *U*-test: **P* < 0.05. Lower: The population in each phase of cell cycle was assessed by fluorescence-activated cell sorting using HO-1-N-1 cell line 72 h after transfection of *PRTFDC1*-siRNA or *Luc*-siRNA. The data presented are the means \pm s.d. of triplicate experiments. Statistical analysis used the Mann-Whitney *U*-test: **P* < 0.05.

(<http://www.ebi.ac.uk/emboss/cpgplot/>) and fragments containing part of Fragment 1 (Fragments 2 and 3 in Figure 3a) were obtained by genomic PCR, and ligated into the pGL3-Basic vector (Promega, Madison, WI, USA). Reporter assay was performed as described elsewhere (Sonoda *et al.*, 2004) using each construct or a control empty vector and an internal control pRL-hTK vector (Promega).

COBRA and bisulfite sequencing

Genomic DNAs were treated with sodium bisulfite, and subjected to PCR using primer sets designed to amplify the regions of interest, which were divided into two

PCR fragments to analyse the entire sequences effectively (Supplementary Table S2). For COBRA, PCR products were digested with *MluI* or *TaqI* and electrophoresed (Xiong and Laird, 1997). For bisulfite sequencing, the PCR products were subcloned and then sequenced.

Transient transfection, western blotting and colony-formation assays

Two plasmids expressing C-terminally 3 \times Myc-tagged *PRTFDC1* (pCMV-3Tag4A-*PRTFDC1*) were obtained by cloning a full coding sequence of *PRTFDC1* into the pCMV-3Tag4A vector (Stratagene, La Jolla, CA, USA) in-frame

along with the Myc-epitope. pCMV-3Tag4A-PRTFDC1 or the empty vector (pCMV-3Tag4A-mock) control, were transfected into cells for colony formation assays as described elsewhere (Sonoda *et al.*, 2004). The expression of PRTFDC1 protein in transiently transfected cells was confirmed 36 h after transfection by western blot analysis using anti-Myc antibody (Cell Signaling Technology, Beverly, MA, USA), as described elsewhere (Imoto *et al.*, 2006). After 3 weeks of incubation with appropriate concentrations of G418 in six-well plates or 100-mm culture dishes, cells were fixed with 70% ethanol and stained with crystal violet.

Transfection with synthetic small interfering RNA

PRTFDC1-specific siRNA (PRTFDC1-siRNA) was purchased from Dharmacon (Lafayette, CO, USA). A control siRNA for the luciferase gene (CGUACGCGGAAUACUUCGA, *Luc*-siRNA) was synthesized by Sigma. Each siRNA (50 nM) was transfected into OSCC cells (St. Louis, MO, USA) using Lipofectamine 2000 (Invitrogen) according to the manufacturer's instructions. The numbers of viable cells 24–96 h after

transfection were assessed by a colorimetric water-soluble tetrazolium salt (WST) assay as described elsewhere (Saigusa *et al.*, 2007). The cell cycle was analysed using FACS as described elsewhere (Saigusa *et al.*, 2007).

Acknowledgements

We are grateful to Professor Yusuke Nakamura (Human Genome Center, The Institute of Medical Science, The University of Tokyo) for his continuous encouragement throughout this work. We thank Ai Watanabe, Ayako Takahashi and Rumi Mori for technical assistance. This work was supported by Grants-in-Aid for Scientific Research on Priority Areas (C) and 21st Century Center of Excellence Program for Molecular Destruction and Reconstitution of Tooth and Bone from the Ministry of Education, Culture, Sports, Science and Technology, Japan; and by a Grant-in-Aid from Core Research for Evolutional Science and Technology (CREST) of the Japan Science and Technology Corporation (JST).

References

- Akanuma D, Uzawa N, Yoshida MA, Negishi A, Amagasa T, Ikeuchi T. (1999). Inactivation patterns of the p16 (INK4a) gene in oral squamous cell carcinoma cell lines. *Oral Oncol* **35**: 476–483.
- Baldwin C, Garnis C, Zhang L, Rosin MP, Lam WL. (2005). Multiple microalterations detected at high frequency in oral cancer. *Cancer Res* **65**: 7561–7567.
- Brinkman BM, Wong DT. (2006). Disease mechanism and biomarkers of oral squamous cell carcinoma. *Curr Opin Oncol* **18**: 228–233.
- Friend SH, Bernards R, Rogelj S, Weinberg RA, Rapaport JM, Albert DM *et al.* (1986). A human DNA segment with properties of the gene that predisposes to retinoblastoma and osteosarcoma. *Nature (London)* **323**: 643–646.
- Fujimoto R, Kamata N, Yokoyama K, Taki M, Tomonari M, Tsutsumi S *et al.* (2002). Establishment of immortalized human oral keratinocytes by gene transfer of a telomerase component. *J Jpn Oral Muco Membr (Japanese)* **8**: 1–8.
- Ha PK, Califano JA. (2006). Promoter methylation and inactivation of tumour-suppressor genes in oral squamous-cell carcinoma. *Lancet Oncol* **7**: 77–82.
- Hahn SA, Schutte M, Hoque AT, Moskaluk CA, da Costa LT, Rozenblum E *et al.* (1996). DPC4, a candidate tumor suppressor gene at human chromosome 18q21.1. *Science (Wash. DC)* **271**: 350–353.
- Hermesen MA, Joenje H, Arwert F, Braakhuis BJ, Baak JP, Westerveld A *et al.* (1997). Assessment of chromosomal gains and losses in oral squamous cell carcinoma by comparative genomic hybridisation. *Oral Oncol* **33**: 414–418.
- Imoto I, Izumi H, Yokoi S, Hosoda H, Shibata T, Hosoda F *et al.* (2006). Frequent silencing of the candidate tumor suppressor PCDH20 by epigenetic mechanism in non-small-cell lung cancers. *Cancer Res* **66**: 4617–4626.
- Inazawa J, Inoue J, Imoto I. (2004). Comparative genomic hybridization (CGH)-arrays pave the way for identification of novel cancer-related genes. *Cancer Sci* **95**: 559–563.
- Izumi H, Inoue J, Yokoi S, Hosoda H, Shibata T, Sunamori M *et al.* (2005). Frequent silencing of DBC1 is by genetic or epigenetic mechanisms in non-small cell lung cancers. *Hum Mol Genet* **14**: 997–1007.
- Jin C, Jin Y, Wennerberg J, Annertz K, Enoksson J, Mertens F. (2006). Cytogenetic abnormalities in 106 oral squamous cell carcinomas. *Cancer Genet Cytogenet* **164**: 44–53.
- Jones PA, Baylin SB. (2002). The fundamental role of epigenetics events in cancer. *Nat Rev Genet* **3**: 415–428.
- Kamb A, Gruis NA, Weaver-Feldhaus J, Liu Q, Harshman K, Tavitgian SV *et al.* (1994). A cell cycle regulator potentially involved in genesis of many tumor types. *Science (Wash DC)* **264**: 436–440.
- Kolb A. (2003). The first intron of the murine β -casein gene contains a functional promoter. *Biochem Biophys Res Commun* **306**: 1099–1105.
- Kusumoto Y, Hirano H, Saitoh K, Yamada S, Takedachi M, Nozaki T *et al.* (2004). Human gingival epithelial cells produce chemotactic factors Interleukin-8 and Monocyte Chemoattractant Protein-1 after stimulation with *Porphyromonas gingivalis* via Toll-Like Receptor 2. *J Periodontol* **75**: 370–378.
- Li J, Yen C, Liaw D, Podsypanina K, Bose S, Wang SI *et al.* (1997). PTEN, a putative protein tyrosine phosphatase gene mutated in human brain, breast, and prostate cancer. *Science (Wash. DC)* **275**: 1943–1947.
- Misawa A, Inoue J, Sugino Y, Hosoi H, Sugimoto T, Hosoda F *et al.* (2005). Methylation-associated silencing of the nuclear receptor 112 gene in advanced-type neuroblastomas, identified by bacterial artificial chromosome array-based methylated CpG island amplicon. *Cancer Res* **65**: 10233–10242.
- Nagpal JK, Das BR. (2003). Oral cancer: reviewing the present understanding of its molecular mechanism and exploring the future directions for its effective management. *Oral Oncol* **39**: 213–221.
- Nakagawachi T, Soejima H, Urano T, Zhao W, Higashimoto K, Satoh Y *et al.* (2003). Silencing effect of CpG island hypermethylation and histone modifications on O6-methyl-guanine-DNA methyltransferase (MGMT) gene expression in human cancer. *Oncogene* **22**: 8835–8844.
- Nicklas JA. (2006). Pseudogenes of the human HPRT1 gene. *Environ Mol Mutagen* **47**: 212–218.
- Parkin DM, Bray F, Ferlay J, Pisani P. (2005). Global cancer statistics, 2002. *CA Cancer J Clin* **55**: 74–108.
- Saigusa K, Imoto I, Tanikawa C, Aoyagi M, Ohno K, Nakamura Y *et al.* (2007). RGC32, a novel p53-inducible gene, is located on centrosomes during mitosis and results in G2/M arrest. *Oncogene* **26**: 1110–1121.
- Scully C, Field JK, Tanzawa H. (2000). Genetic aberrations in oral or head and neck squamous cell carcinoma (SCCHN).

- I. Carcinogen metabolism, DNA repair and cell cycle control. *Oral Oncol* **36**: 256–263.
- Shaw R. (2006). The epigenetics of oral cancer. *Int J Oral Maxillofac Surg* **35**: 101–108.
- Snijders AM, Nowak N, Seagraves R, Blackwood S, Brown N, Conroy J *et al.* (2001). Assembly of microarrays for genome-wide measurement of DNA copy number. *Nat Genet* **29**: 263–264.
- Snijders AM, Schmidt BL, Fridlyand J, Dekker N, Pinkel D, Jordan RC *et al.* (2005). Rare amplicons implicate frequent deregulation of cell fate specification pathways in oral squamous cell carcinoma. *Oncogene* **24**: 4232–4242.
- Sonoda I, Imoto I, Inoue J, Shibata T, Shimada Y, Chin K *et al.* (2004). Frequent silencing of low density lipoprotein receptor-related protein 1B (LRP1B) expression by genetic and epigenetic mechanisms in esophageal squamous cell carcinoma. *Cancer Res* **64**: 3741–3747.
- Takada H, Imoto I, Tsuda H, Nakanishi Y, Ichikura T, Mochizuki H *et al.* (2005b). ADAM23, a possible tumor suppressor gene, is frequently silenced in gastric cancers by homozygous deletion or aberrant promoter hypermethylation. *Oncogene* **24**: 8051–8060.
- Takada H, Imoto I, Tsuda H, Nakanishi Y, Sakakura C, Mitsufuji S *et al.* (2006). Genomic loss and epigenetic silencing of very-low-density lipoprotein receptor involved in gastric carcinogenesis. *Oncogene* **25**: 6554–6562.
- Takada H, Imoto I, Tsuda H, Sonoda I, Ichikura T, Mochizuki H *et al.* (2005a). Screening of DNA copy-number aberrations in gastric cancer cell lines by array-based comparative genomic hybridization. *Cancer Sci* **96**: 100–110.
- Wolff E, Girod S, Liehr T, Vorderwulbecke U, Ries J, Steininger H *et al.* (1998). Oral squamous cell carcinomas are characterized by a rather uniform pattern of genomic imbalances detected by comparative genomic hybridisation. *Oral Oncol* **34**: 186–190.
- Xiong Z, Laird PW. (1997). COBRA: a sensitive and quantitative DNA methylation assay. *Nucleic Acids Res* **25**: 2532–2534.

Supplementary Information accompanies the paper on the Oncogene website (<http://www.nature.com/onc>).